

Model Risk for Exotic and Moment Derivatives

Wim Schoutens*
Erwin Simons[†]
Jurgen Tistaert[‡]
§

September 4, 2004

*K.U.Leuven, Celestijnenlaan 200 B, B-3001 Leuven, Belgium. E-mail: Wim.Schoutens@wis.kuleuven.ac.be

[†]ING SWE, Financial Modeling, Marnixlaan 24, B-1000 Brussels, Belgium. E-mail: Erwin.Simons@ing.be

[‡]ING SWE, Financial Modeling, Marnixlaan 24, B-1000 Brussels, Belgium. E-mail: Jurgen.Tistaert@ing.be

[§]The authors note that the current paper does not necessarily reflect the views of their employer.

Abstract

We show that several advanced equity option models incorporating stochastic volatility can be calibrated very nicely to a realistic implied volatility surface. More specifically, we focus on the Heston Stochastic Volatility model (with and without jumps in the stock price process), the Barndorff-Nielsen-Shephard model and Lévy models with stochastic time. All these models are capable of accurately describing the marginal distribution of stock prices or indices and hence lead to almost identical European vanilla option prices. As such, we can hardly discriminate between the different processes on the basis of their smile-conform pricing characteristics. We therefore are tempted applying them to a range of exotics. However, due to the different structure in path-behaviour between these models, we find that the resulting exotics prices can vary significantly. We subsequently introduce *moment derivatives*. These are derivatives that depend on the realized moments of (daily) logreturns. An already traded example of these derivatives is the Variance Swap. We show how to hedge these options and calculate their prices by Monte-Carlo simulation. A comparison of these moment derivatives premiums demonstrates an even bigger discrepancy between the aforementioned models. It motivates a further study on how to model the fine stochastic behaviour of assets over time.

1 Introduction

Since the seminal publication of the Black-Scholes model in 1973, we have witnessed a vast effort to relax a number of its restrictive assumptions. Empirical data show evidence for non-normal distributed log-returns together with the presence of stochastic volatility. Nowadays, a battery of models are available which capture non-normality and integrate stochastic volatility. We focus on the following advanced models: the Heston Stochastic Volatility Model [16] and its generalization allowing for jumps in the stock price process (see e.g. [1]), the Barndorff-Nielsen-Shephard model introduced in [2] and Lévy models with stochastic time introduced by Carr, Geman, Madan and Yor [9]. This class of models are build out of a Lévy process which is time-changed by a stochastic clock. The latter induces the desired stochastic volatility effect.

Our paper continues along the lines of Hull e.a. [18] and Hirsa e.a. [17] and their study on the effect of model risk on the pricing of exotic options is extended in various aspects. The current paper is organised as follows. Section 2 elaborates on the technical details of the models and we state each of the closed-form characteristic functions. The latter are the necessary ingredients for a calibration procedure, which is tackled in section 3. The pricing of the options in that framework is based on the analytical formula of Carr and Madan [8]. We will show that all of the above models can be calibrated very well to a representative set of European call options. Section 4 describes the simulation algorithms for the stochastic processes involved. Armed with good calibration results and powerful simulation tools, we will price a range of exotics. Section 5 presents the computational results for digital barriers, one-touch barriers, lookbacks and cliquet options under the different models. While the European vanilla option prices hardly differ across all models considered, we obtain significant differences in the prices of the exotics. These observations sparked our interest to push this study further in section 6 by introducing and pricing moment derivatives. We extend a hedging formula as proposed by Carr and Lewis [7]. More precisely, we show how to hedge the realized k th moment swap by a dynamic trading strategy in bonds and stocks, a static position in vanilla options and a static position in the realized moment swaps of lower order. The paper concludes with a formal discussion and gives some directions for further research.

2 The Models

We consider the risk-neutral dynamics of the different models. Let us shortly define some concepts and introduce their notation.

Let $S = \{S_t, 0 \leq t \leq T\}$ denote the stock price process and $\phi(u, t)$ the characteristic function of the random variable $\log S_t$, i.e.,

$$\phi(u, t) = E[\exp(iu \log(S_t))].$$

If for every integer n , $\phi(u, t)$ is also the n th power of a characteristic function, we say that the distribution is *infinitely divisible*. A Lévy process $X = \{X_t, t \geq 0\}$

is a stochastic process which starts at zero and has independent and stationary increments such that the distribution of the increment is an infinitely divisible distribution. A *subordinator* is a nonnegative nondecreasing Lévy process. A general reference on Lévy processes is [5], for applications in finance see [24].

The risk-free continuously compound interest rate is assumed to be constant and denoted by r . The dividend yield is also assumed to be constant and denoted by q .

2.1 The Heston Stochastic Volatility Model

The stock price process in the Heston Stochastic Volatility model (HEST) follows the Black-Scholes SDE in which the volatility is behaving stochastically over time:

$$\frac{dS_t}{S_t} = (r - q)dt + \sigma_t dW_t, \quad S_0 \geq 0,$$

with the (squared) volatility following the classical Cox-Ingersoll-Ross (CIR) process:

$$d\sigma_t^2 = \kappa(\eta - \sigma_t^2)dt + \theta\sigma_t d\tilde{W}_t, \quad \sigma_0 \geq 0,$$

where $W = \{W_t, t \geq 0\}$ and $\tilde{W} = \{\tilde{W}_t, t \geq 0\}$ are two correlated standard Brownian motions such that $\text{Cov}[dW_t d\tilde{W}_t] = \rho dt$.

The characteristic function $\phi(u, t)$ is in this case given by (see [16] or [1]):

$$\begin{aligned} \phi(u, t) &= E[\exp(iu \log(S_t)) | S_0, \sigma_0^2] \\ &= \exp(iu(\log S_0 + (r - q)t)) \\ &\quad \times \exp(\eta\kappa\theta^{-2}((\kappa - \rho\theta ui - d)t - 2\log((1 - ge^{-dt})/(1 - g)))) \\ &\quad \times \exp(\sigma_0^2\theta^{-2}(\kappa - \rho\theta ui - d)(1 - e^{-dt})/(1 - ge^{-dt})), \end{aligned}$$

where

$$d = ((\rho\theta ui - \kappa)^2 - \theta^2(-iu - u^2))^{1/2}, \quad (1)$$

$$g = (\kappa - \rho\theta ui - d)/(\kappa - \rho\theta ui + d). \quad (2)$$

2.2 The Heston Stochastic Volatility Model with Jumps

An extension of HEST introduces jumps in the asset price [1]. Jumps occur as a Poisson process and the percentage jump-sizes are lognormally distributed. An extension also allowing jumps in the volatility was described in [20]. We opt to focus on the continuous version and the one with jumps in the stock price process only.

In the Heston Stochastic Volatility model with jumps (HESJ), the SDE of the stock price process is extended to yield:

$$\frac{dS_t}{S_t} = (r - q - \lambda\mu_J)dt + \sigma_t dW_t + J_t dN_t, \quad S_0 \geq 0,$$

where $N = \{N_t, t \geq 0\}$ is an independent Poisson process with intensity parameter $\lambda > 0$, i.e. $E[N_t] = \lambda t$. J_t is the percentage jump size (conditional on a jump occurring) that is assumed to be lognormally, identically and independently distributed over time, with unconditional mean μ_J . The standard deviation of $\log(1 + J_t)$ is σ_J :

$$\log(1 + J_t) \sim \text{Normal} \left(\log(1 + \mu_J) - \frac{\sigma_J^2}{2}, \sigma_J^2 \right);$$

The SDE of (squared) volatility process remains unchanged:

$$d\sigma_t^2 = \kappa(\eta - \sigma_t^2)dt + \theta\sigma_t d\tilde{W}_t, \quad \sigma_0 \geq 0,$$

where $W = \{W_t, t \geq 0\}$ and $\tilde{W} = \{\tilde{W}_t, t \geq 0\}$ are two correlated standard Brownian motions such that $\text{Cov}[dW_t d\tilde{W}_t] = \rho dt$. Finally, J_t and N are independent, as well as of W and of \tilde{W} .

The characteristic function $\phi(u, t)$ is in this case given by:

$$\begin{aligned} \phi(u, t) &= E[\exp(iu \log(S_t)) | S_0, \sigma_0^2] \\ &= \exp(iu(\log S_0 + (r - q)t)) \\ &\quad \times \exp(\eta\kappa\theta^{-2}((\kappa - \rho\theta iu - d)t - 2\log((1 - ge^{-dt})/(1 - g)))) \\ &\quad \times \exp(\sigma_0^2\theta^{-2}(\kappa - \rho\theta iu - d)(1 - e^{-dt})/(1 - ge^{-dt})), \\ &\quad \times \exp(-\lambda\mu_J iut + \lambda t((1 + \mu_J)^{iu} \exp(\sigma_J^2(iu/2)(iu - 1)) - 1)), \end{aligned}$$

where d and g are as in (1) and (2).

2.3 The Barndorff-Nielsen-Shephard Model

This class of models, denoted by BN-S, were introduced in [2] and have a comparable structure to HEST. The volatility is now modeled by an Ornstein Uhlenbeck (OU) process driven by a subordinator. We use the classical and tractable example of the Gamma-OU process. The marginal law of the volatility is Gamma-distributed. Volatility can only jump upwards and then it will decay exponentially. A co-movement effect between up-jumps in volatility and (down)-jumps in the stock price is also incorporated. The price of the asset will jump downwards when an up-jump in volatility takes place. In the absence of a jump, the asset price process moves continuously and the volatility decays also continuously. Other choices for OU-processes can be made, we mention especially the Inverse Gaussian OU process, leading also to a tractable model.

The squared volatility now follows a SDE of the form:

$$d\sigma_t^2 = -\lambda\sigma_t^2 dt + dz_{\lambda t}, \quad (3)$$

where $\lambda > 0$ and $z = \{z_t, t \geq 0\}$ is a subordinator as introduced before.

The risk-neutral dynamics of the log-price $Z_t = \log S_t$ are given by:

$$dZ_t = (r - q - \lambda k(-\rho) - \sigma_t^2/2)dt + \sigma_t dW_t + \rho dz_{\lambda t}, \quad Z_0 = \log S_0,$$

where $W = \{W_t, t \geq 0\}$ is a Brownian motion independent of $z = \{z_t, t \geq 0\}$ and where $k(u) = \log E[\exp(-uz_1)]$ is the cumulant function of z_1 . Note that the parameter ρ is introducing a co-movement effect between the volatility and the asset price process.

As stated above, we chose the Gamma-OU process. For this process $z = \{z_t, t \geq 0\}$ is a compound-Poisson process:

$$z_t = \sum_{n=1}^{N_t} x_n, \quad (4)$$

where $N = \{N_t, t \geq 0\}$ is a Poisson process with intensity parameter a , i.e. $E[N_t] = at$ and $\{x_n, n = 1, 2, \dots\}$ is an independent and identically distributed sequence, and each x_n follows an exponential law with mean $1/b$. One can show that the process $\sigma^2 = \{\sigma_t^2, t \geq 0\}$ is a stationary process with a marginal law that follows a Gamma distribution with mean a and variance a/b . This means that if one starts the process with an initial value sampled from this Gamma distribution, at each future time point t , σ_t^2 is also following that Gamma distribution. Under this law, the cumulant function reduces to:

$$k(u) = \log E[\exp(-uz_1)] = -au(b+u)^{-1}.$$

In this case, one can write the characteristic function [3] of the log price in the form:

$$\begin{aligned} \phi(u, t) &= E[\exp(iu \log S_t) | S_0, \sigma_0] \\ &= \exp(iu(\log(S_0) + (r - q - a\lambda\rho(b - \rho)^{-1})t)) \\ &\quad \times \exp(-\lambda^{-1}(u^2 + iu)(1 - \exp(-\lambda t))\sigma_0^2/2) \\ &\quad \times \exp\left(a(b - f_2)^{-1} \left(b \log\left(\frac{b - f_1}{b - iu\rho}\right) + f_2\lambda t\right)\right), \end{aligned}$$

where

$$\begin{aligned} f_1 = f_1(u) &= iu\rho - \lambda^{-1}(u^2 + iu)(1 - \exp(-\lambda t))/2, \\ f_2 = f_2(u) &= iu\rho - \lambda^{-1}(u^2 + iu)/2. \end{aligned}$$

2.4 Lévy Models with Stochastic Time

Another way to build in stochastic volatility effects is by making time stochastic. Periods with high volatility can be looked at as if time runs faster than in periods with low volatility. Applications of stochastic time change to asset pricing go back to Clark [10], who models the asset price as a geometric Brownian motion time-changed by an independent Lévy subordinator.

The Lévy models with stochastic time considered in this paper are build out of two independent stochastic processes. The first process is a Lévy process. The behaviour of the asset price will be modeled by the exponential of the Lévy

process suitably time-changed. Typical examples are the Normal distribution, leading to the Brownian motion, the Normal Inverse Gaussian (NIG) distribution, the Variance Gamma (VG) distribution, the (generalized) hyperbolic distribution, the Meixner distribution, the CGMY distribution and many others. An overview can be found in [24]. We opt to work with the VG and NIG processes for which simulation issues become quite standard.

The second process is a stochastic clock that builds in a stochastic volatility effect by making time stochastic. The above mentioned (first) Lévy process will be subordinated (or time-changed) by this stochastic clock. By definition of a subordinator, the time needs to increase and the process modeling the rate of time change $y = \{y_t, t \geq 0\}$ needs also to be positive. The economic time elapsed in t units of calendar time is then given by the integrated process $Y = \{Y_t, t \geq 0\}$ where

$$Y_t = \int_0^t y_s ds.$$

Since y is a positive process, Y is an increasing process. We investigate two processes y which can serve for the rate of time change: the CIR process (continuous) and the Gamma-OU process (jump process).

We first discuss NIG and VG and subsequently introduce the stochastic clocks CIR and Gamma-OU. In order to model the stock price process as a time changed Lévy process, one needs the link between the stochastic clock and the Lévy process. This role will be fulfilled by the characteristic function enclosing both independent processes as described at the end of this section.

NIG Lévy Process: A NIG process is based on the Normal Inverse Gaussian (NIG) distribution, $\text{NIG}(\alpha, \beta, \delta)$, with parameters $\alpha > 0$, $-\alpha < \beta < \alpha$ and $\delta > 0$. Its characteristic function is given by:

$$\phi_{\text{NIG}}(u; \alpha, \beta, \delta) = \exp\left(-\delta\left(\sqrt{\alpha^2 - (\beta + iu)^2} - \sqrt{\alpha^2 - \beta^2}\right)\right).$$

Since this is an infinitely divisible characteristic function, one can define the NIG-process $X^{(\text{NIG})} = \{X_t^{(\text{NIG})}, t \geq 0\}$, with $X_0^{(\text{NIG})} = 0$, as the process having stationary and independent NIG distributed increments. So, an increment over the time interval $[s, s + t]$ follows a $\text{NIG}(\alpha, \beta, \delta t)$ law. A NIG-process is a pure jump process. One can relate the NIG process to an Inverse Gaussian time-changed Brownian motion, which is particularly useful for simulation issues (see section 4.1).

VG Lévy Process: The characteristic function of the $\text{VG}(C, G, M)$, with parameters $C > 0$, $G > 0$ and $M > 0$ is given by:

$$\phi_{\text{VG}}(u; C, G, M) = \left(\frac{GM}{GM + (M - G)iu + u^2}\right)^C.$$

This distribution is infinitely divisible and one can define the VG-process $X^{(\text{VG})} = \{X_t^{(\text{VG})}, t \geq 0\}$ as the process which starts at zero, has independent and stationary increments and where the increment $X_{s+t}^{(\text{VG})} - X_s^{(\text{VG})}$ over the time interval

$[s, s + t]$ follows a $\text{VG}(Ct, G, M)$ law. In [21], it was shown that the VG-process may also be expressed as the difference of two independent Gamma processes, which is helpful for simulation issues (see Section 4.2).

CIR Stochastic Clock: Carr, Geman, Madan and Yor [9] use as the rate of time change the CIR process that solves the SDE:

$$dy_t = \kappa(\eta - y_t)dt + \lambda y_t^{1/2}dW_t,$$

where $W = \{W_t, t \geq 0\}$ is a standard Brownian motion. The characteristic function of Y_t (given y_0) is explicitly known (see [13]):

$$\begin{aligned} \varphi_{CIR}(u, t; \kappa, \eta, \lambda, y_0) &= E[\exp(iuY_t)|y_0] \\ &= \frac{\exp(\kappa^2 \eta t / \lambda^2) \exp(2y_0 i u / (\kappa + \gamma \coth(\gamma t / 2)))}{(\cosh(\gamma t / 2) + \kappa \sinh(\gamma t / 2) / \gamma)^{2\kappa \eta / \lambda^2}}, \end{aligned}$$

where

$$\gamma = \sqrt{\kappa^2 - 2\lambda^2 i u}.$$

Gamma-OU Stochastic Clock: The rate of time change is now a solution of the SDE:

$$dy_t = -\lambda y_t dt + dz_{\lambda t}, \quad (5)$$

where the process $z = \{z_t, t \geq 0\}$ is as in (4) a compound Poisson process. In the Gamma-OU case the characteristic function of Y_t (given y_0) can be given explicitly.

$$\begin{aligned} \varphi_{\Gamma-OU}(u; t, \lambda, a, b, y_0) &= E[\exp(iuY_t)|y_0] \\ &= \exp\left(iu y_0 \lambda^{-1} (1 - e^{-\lambda t}) + \frac{\lambda a}{iu - \lambda b} \left(b \log\left(\frac{b}{b - iu \lambda^{-1} (1 - e^{-\lambda t})}\right) - iut\right)\right). \end{aligned}$$

Time Changed Lévy Process: Let $Y = \{Y_t, t \geq 0\}$ be the process we choose to model our business time (remember that Y is the integrated process of y). Let us denote by $\varphi(u; t, y_0)$ the characteristic function of Y_t given y_0 . The (risk-neutral) price process $S = \{S_t, t \geq 0\}$ is now modeled as follows:

$$S_t = S_0 \frac{\exp((r - q)t)}{E[\exp(X_{Y_t})|y_0]} \exp(X_{Y_t}), \quad (6)$$

where $X = \{X_t, t \geq 0\}$ is a Lévy process. The factor $\exp((r - q)t) / E[\exp(X_{Y_t})|y_0]$ puts us immediately into the risk-neutral world by a mean-correcting argument. Basically, we model the stock price process as the ordinary exponential of a time-changed Lévy process. The process incorporates jumps (through the Lévy

process X_t) and stochastic volatility (through the time change Y_t). The characteristic function $\phi(u, t)$ for the log of our stock price is given by:

$$\begin{aligned}\phi(u, t) &= E[\exp(iu \log(S_t)) | S_0, y_0] \\ &= \exp(iu((r - q)t + \log S_0)) \frac{\varphi(-i\psi_X(u); t, y_0)}{\varphi(-i\psi_X(-i); t, y_0)^{iu}},\end{aligned}\quad (7)$$

where

$$\psi_X(u) = \log E[\exp(iuX_1)];$$

$\psi_X(u)$ is called the characteristic exponent of the Lévy process.

Since we consider two Lévy processes (VG and NIG) and two stochastic clocks (CIR and Gamma-OU), we will finally end up with four resulting models abbreviated as VG-CIR, VG-OUG, NIG-CIR and NIG-OUG.

Because of (time)-scaling effects, one can set $y_0 = 1$, and scale the present rate of time change to one. More precisely, we have that the characteristic function $\phi(u, t)$ of (7) satisfies:

$$\begin{aligned}\phi_{NIG-CIR}(u, t; \alpha, \beta, \delta, \kappa, \eta, \lambda, y_0) &= \phi_{NIG-CIR}(u, t; \alpha, \beta, \delta y_0, \kappa, \eta/y_0, \lambda/\sqrt{y_0}, 1), \\ \phi_{NIG-\Gamma OU}(u, t; \alpha, \beta, \delta, \lambda, a, b, y_0) &= \phi_{NIG-\Gamma OU}(u, t; \alpha, \beta, \delta y_0, \lambda, a, b y_0, 1), \\ \phi_{VG-CIR}(u, t; C, G, M, \kappa, \eta, \lambda, y_0) &= \phi_{VG-CIR}(u, t; C y_0, G, M, \kappa, \eta/y_0, \lambda/\sqrt{y_0}, 1), \\ \phi_{VG-\Gamma OU}(u, t; C, G, M, \lambda, a, b, y_0) &= \phi_{VG-\Gamma OU}(u, t; C y_0, G, M, \lambda, a, b y_0, 1).\end{aligned}$$

Actually, this time-scaling effect lies at the heart of the idea of incorporating stochastic volatility through making time stochastic. Here, it comes down to the fact that instead of making the volatility parameter (of the Black-Scholes model) stochastic, we are making the parameter δ in the NIG case and the parameter C in the VG case stochastic (via the time). Note that this effect does not only influence the standard deviation (or volatility) of the processes, also the skewness and the kurtosis are now fluctuating stochastically.

3 Calibration

Carr and Madan [8] developed pricing methods for the classical vanilla options which can be applied in general when the characteristic function of the risk-neutral stock price process is known.

Let α be a positive constant such that the α th moment of the stock price exists. For all stock price models encountered here, typically a value of $\alpha = 0.75$ will do fine. Carr and Madan then showed that the price $C(K, T)$ of a European call option with strike K and time to maturity T is given by:

$$C(K, T) = \frac{\exp(-\alpha \log(K))}{\pi} \int_0^{+\infty} \exp(-iv \log(K)) \varrho(v) dv, \quad (8)$$

where

$$\varrho(v) = \frac{\exp(-rT) E[\exp(i(v - (\alpha + 1)i) \log(S_T))]}{\alpha^2 + \alpha - v^2 + i(2\alpha + 1)v} \quad (9)$$

$$= \frac{\exp(-rT)\phi(v - (\alpha + 1)i, T)}{\alpha^2 + \alpha - v^2 + i(2\alpha + 1)v}. \quad (10)$$

Using Fast Fourier Transforms, one can compute within a second the complete option surface on an ordinary computer. We apply the above calculation method in our calibration procedure and estimate the model parameters by minimizing the difference between market prices and model prices in a least-squares sense.

The data set consists of 144 plain vanilla call option prices with maturities ranging from less than one month up to 5.16 years. These prices are based on the implied volatility surface of the Eurostoxx 50 index, having a value of 2461.44 on October 7th, 2003. The volatilities can be found in table 8. For the sake of simplicity and to focus on the essence of the stochastic behaviour of the asset, we set the risk-free interest rate equal to 3 percent and the dividend yield to zero.

Contrary to the approach described in [17], we search for a single global set of parameters per model which we fit (and which captures smile information) across the full range of maturities in the data set. This global parameter set can then be used to price path dependent derivatives (e.g. payoffs at multiple points during its lifetime or moment derivatives, see section 6 and 7). This in contrast with the parameter set resulting from a fitting procedure at a single maturity date, which can in principle only be used to price option payoffs occurring at that specific maturity.

The results of the global calibration are visualized in Figure 1 and Figure 2 for the NIG-CIR and the BNS model respectively. The other models give rise to completely similar figures. Here, the circles are the market prices and the plus signs are the analytical prices (calculated through formula (8) using the respective characteristic functions and obtained parameters).

In Table 1 one finds the risk-neutral parameters for the different models. For comparative purposes, one computes several global measures of fit. We consider the root mean square error (*rmse*), the average absolute error as a percentage of the mean price (*ape*), the average absolute error (*aae*) and the average relative percentage error (*arpe*):

$$\begin{aligned} rmse &= \sqrt{\sum_{options} \frac{(\text{Market price} - \text{Model price})^2}{\text{number of options}}} \\ ape &= \frac{1}{\text{mean option price}} \sum_{options} \frac{|\text{Market price} - \text{Model price}|}{\text{number of options}} \\ aae &= \sum_{options} \frac{|\text{Market price} - \text{Model price}|}{\text{number of options}} \\ arpe &= \frac{1}{\text{number of options}} \sum_{options} \frac{|\text{Market price} - \text{Model price}|}{\text{Market price}} \end{aligned}$$

In Table 2 an overview of these measures of fit are given.

HEST
$\sigma_0^2 = 0.0654, \kappa = 0.6067, \eta = 0.0707, \theta = 0.2928, \rho = -0.7571$
HESJ
$\sigma_0^2 = 0.0576, \kappa = 0.4963, \eta = 0.0650, \theta = 0.2286, \rho = -0.9900, \mu_j = 0.1791,$ $\sigma_j = 0.1346, \lambda = 0.1382$
BN-S
$\rho = -4.6750, \lambda = 0.5474, b = 18.6075, a = 0.6069, \sigma_0^2 = 0.0433$
VG-CIR
$C = 18.0968, G = 20.0276, M = 26.3971, \kappa = 1.2145, \eta = 0.5501,$ $\lambda = 1.7913, y_0 = 1$
VG-OUT
$C = 6.1610, G = 9.6443, M = 16.0260, \lambda = 1.6790, a = 0.3484,$ $b = 0.7664, y_0 = 1$
NIG-CIR
$\alpha = 16.1975, \beta = -3.1804, \delta = 1.0867, \kappa = 1.2101, \eta = 0.5507,$ $\lambda = 1.7864, y_0 = 1$
NIG-OUT
$\alpha = 8.8914, \beta = -3.1634, \delta = 0.6728, \lambda = 1.7478, a = 0.3442,$ $b = 0.7628, y_0 = 1$

Table 1: Risk Neutral Parameters

4 Simulation

In the current section we describe in some detail how the particular processes presented in section 2 can be implemented in practice in a Monte-Carlo simulation pricing framework. For this we first discuss the numerical implementation of the four building block processes which drive them. This will be followed by an explanation of how one assembles a time-changed Lévy process.

4.1 NIG Lévy Process

To simulate a NIG process, we first describe how to simulate $\text{NIG}(\alpha, \beta, \delta)$ random numbers. NIG random numbers can be obtained by mixing Inverse

Model:	rmse	ape	aae	arpe
HEST	3.0281	0.0048	2.4264	0.0174
HESJ	2.8101	0.0045	2.2469	0.0126
BN-S	3.5156	0.0056	2.8194	0.0221
VG-CIR	2.3823	0.0038	1.9337	0.0106
VG-OUT	3.4351	0.0056	2.8238	0.0190
NIG-CIR	2.3485	0.0038	1.9194	0.0099
NIG-OUT	3.2737	0.0054	2.7385	0.0175

Table 2: Global fit error measures

Gaussian (IG) random numbers and standard Normal numbers in the following manner. An IG(a, b) random variable X has a characteristic function given by:

$$E[\exp(iuX)] = \exp(-a\sqrt{-2ui + b^2} - b)$$

First simulate IG($1, \delta\sqrt{\alpha^2 - \beta^2}$) random numbers i_k , for example using the Inverse Gaussian generator of Michael, Schucany and Haas [15]. Then sample a sequence of standard Normal random variables u_k . NIG random numbers n_k are then obtained via:

$$n_k = \delta^2\beta i_k + \delta\sqrt{i_k}u_k;$$

Finally the sample paths of a NIG(α, β, δ) process $X = \{X_t, t \geq 0\}$ in the time points $t_n = n\Delta t$, $n = 0, 1, 2, \dots$ can be generated by using the independent NIG($\alpha, \beta, \delta\Delta t$) random numbers n_k as follows:

$$X_0 = 0, \quad X_{t_k} = X_{t_{k-1}} + n_k, \quad k \geq 1.$$

4.2 VG Lévy Process

Since a VG process can be viewed as the difference of two independent Gamma processes, the simulation of a VG process becomes straightforward. A Gamma process with parameters $a, b > 0$ is a Lévy process with Gamma(a, b) distributed increments, i.e. following a Gamma distribution with mean a/b and variance a/b^2 . A VG process $X^{(VG)} = \{X_t^{(VG)}, t \geq 0\}$ with parameters $C, G, M > 0$ can be decomposed as $X_t^{(VG)} = G_t^{(1)} - G_t^{(2)}$, where $G^{(1)} = \{G_t^{(1)}, t \geq 0\}$ is a Gamma process with parameters $a = C$ and $b = M$ and $G^{(2)} = \{G_t^{(2)}, t \geq 0\}$ is a Gamma process with parameters $a = C$ and $b = G$. The generation of Gamma numbers is quite standard. Possible generators are Johnk's gamma generator and Berman's gamma generator [15].

4.3 CIR Stochastic Clock

The simulation of a CIR process $y = \{y_t, t \geq 0\}$ is straightforward. Basically, we discretize the SDE:

$$dy_t = \kappa(\eta - y_t)dt + \lambda y_t^{1/2}dW_t, \quad y_0 \geq 0,$$

where W_t is a standard Brownian motion. Using a first-order accurate explicit differencing scheme in time the sample path of the CIR process $y = \{y_t, t \geq 0\}$ in the time points $t = n\Delta t$, $n = 0, 1, 2, \dots$, is then given by:

$$y_{t_n} = y_{t_{n-1}} + \kappa(\eta - y_{t_{n-1}})\Delta t + \lambda y_{t_{n-1}}^{1/2} \sqrt{\Delta t} v_n,$$

where $\{v_n, n = 1, 2, \dots\}$ is a series of independent standard Normally distributed random numbers. For other more involved simulation schemes, like the Milstein scheme, resulting in a higher-order discretisation in time, we refer to [19].

4.4 Gamma-OU Stochastic Clock

Recall that for the particular choice of a OU-Gamma process the subordinator $z = \{z_t, t \geq 0\}$ in equation (3) is given by the compound Poisson process (4).

To simulate a Gamma(a, b)-OU process $y = \{y_t, t \geq 0\}$ in the time points $t_n = n\Delta t$, $n = 0, 1, 2, \dots$, we first simulate in the same time points a Poisson process $N = \{N_t, t \geq 0\}$ with intensity parameter $a\lambda$. Then (with the convention that an empty sum equals zero)

$$y_{t_n} = (1 - \lambda\Delta t)y_{t_{n-1}} + \sum_{k=N_{t_{n-1}}+1}^{N_{t_n}} x_k \exp(-\lambda\Delta t\tilde{u}_k),$$

where \tilde{u}_k are a series of independent uniformly distributed random numbers and x_k can be obtained from your preferred uniform random number generator via $x_k = -\log(u_k)/b$.

4.5 Path Generation for Time-Changed Lévy Process

The explanation of the building block processes above allow us next to assemble all the parts of the time-changed Lévy process simulation puzzle. For this one can proceed through the following five steps [24]:

- (i) simulate the rate of time change process $y = \{y_t, 0 \leq t \leq T\}$;
- (ii) calculate from (i) the time change $Y = \{Y_t = \int_0^t y_s ds, 0 \leq t \leq T\}$;
- (iii) simulate the Lévy process $X = \{X_t, 0 \leq t \leq Y_T\}$;
- (iv) calculate the time changed Lévy process X_{Y_t} , for $0 \leq t \leq T$;
- (v) calculate the stock price process using (6). The mean correcting factor is calculated as:

$$\frac{\exp((r - q)t)}{E[\exp(X_{Y_t})|y_0]} = \frac{\exp((r - q)t)}{\varphi(-i\psi_X(-i); t, 1)}.$$

5 Pricing of Exotic Options

As evidenced by the quality of the calibration on a set of European call options in section 3, we can hardly discriminate between the different processes on the basis of their smile-conform pricing characteristics. We therefore put the models further to the test by applying them to a range of more exotic options. These range from digital barriers, one-touch barrier options, lookback options and finally cliquet options with local as well as global parameters. These first generation exotics with path-dependent payoffs were selected since they shed more light on the dynamics of the stock processes. At the same time, the pricings

of the cliquet options are highly sensitive to the forward smile characteristics induced by the models.

5.1 Exotic Options

Let us consider contracts of duration T , and denote the maximum and minimum process, resp., of a process $Y = \{Y_t, 0 \leq t \leq T\}$ as

$$M_t^Y = \sup\{Y_u; 0 \leq u \leq t\} \text{ and } m_t^Y = \inf\{Y_u; 0 \leq u \leq t\}, \quad 0 \leq t \leq T.$$

5.1.1 Digital Barriers

We first consider digital barrier options. These options remain worthless unless the stock price hits some predefined barrier level $H > S_0$, in which case they pay at expiry a fixed amount D , normalised to 1 in the current settings. Using risk-neutral valuation, assuming no dividends and a constant interest rate r , the time $t = 0$ price is therefore given by:

$$\text{digital} = e^{-rT} E_Q[1(M_T^S \geq H)],$$

where the expectation is taken under the risk-neutral measure Q .

Observe that with the current definition of digital barriers their pricing reflects exactly the chance of hitting the barrier prior to expiry. The behaviour of the stock after the barrier has been hit does not influence the result, in contrast with the classic barrier options defined below.

5.1.2 One-Touch Barrier Options

For one-touch barrier call options, we focus on the following 4 types:

- The down-and-out barrier call is worthless unless its minimum remains above some "low barrier" H , in which case it retains the structure of a European call with strike K . Its initial price is given by:

$$DOB = e^{-rT} E_Q[(S_T - K)^+ 1(m_T^S > H)]$$

- The down-and-in barrier is a normal European call with strike K , if its minimum went below some "low barrier" H . If this barrier was never reached during the life-time of the option, the option remains worthless. Its initial price is given by:

$$DIB = e^{-rT} E_Q[(S_T - K)^+ 1(m_T^S \leq H)]$$

- The up-and-in barrier is worthless unless its maximum crossed some "high barrier" H , in which case it obtains the structure of a European call with strike K . Its price is given by:

$$UIB = e^{-rT} E_Q[(S_T - K)^+ 1(M_T^S \geq H)]$$

- The up-and-out barrier is worthless unless its maximum remains below some "high barrier" H , in which case it retains the structure of a European call with strike K . Its price is given by:

$$UOB = e^{-rT} E_Q[(S_T - K)^+ 1(M_T^S < H)]$$

5.1.3 Lookback Options

The payoff of a lookback call option corresponds to the difference between the stock price level at expiry S_T and the lowest level it has reached during its lifetime. The time $t = 0$ price of a lookback call option is therefore given by:

$$LC = e^{-rT} E_Q[S_T - m_T^S].$$

Clearly, of the 3 path-dependent options introduced so-far, the lookback option depends the most on the precise path dynamics.

5.1.4 Cliquet Options

Finally we also test the proposed models on the pricing of cliquet options. These still are very popular options in the equity derivatives world that allow the investor to participate (partially) in the performance of an underlying over a series of consecutive time periods $[t_i, t_{i+1}]$ by "clicking in" the sum of these local performances. The local performances are measured relative to the stock level S_{t_i} attained at the start of each new subperiod, and each of the local performances is floored and/or capped to establish whatever desirable mix of positive and/or negative payoff combination. Generally on the final sum an additional global floor (cap) is applied to guarantee a minimum (maximum) overall payoff. This can all be summarised through the following payoff formula:

$$\min \left(cap_{glob}, \max \left(floor_{glob}, \sum_{i=1}^N \min \left(cap_{loc}, \max \left(floor_{loc}, \frac{S_{t_i} - S_{t_{i-1}}}{S_{t_{i-1}}} \right) \right) \right) \right)$$

Observe that the local floor and cap parameters effectively border the relevant "local" price ranges by centering them around the future, and therefore unknown, spot levels S_{t_i} . The pricing will therefore depend in a non-trivial subtle manner on the forward volatility smile dynamics of the respective models, further complicated by the global parameters of the contract. For an in-depth account of the related volatility issues we refer to the contribution of Wilmott [26] in one of the previous issues.

5.2 Exotic Option Prices

We price all exotic options through Monte-Carlo simulation. We consistently average over 1.000.000 simulated paths. All options have a life-time of 3 years. In order to check the accuracy of our simulation algorithm we simulated option

prices for all European calls available in the calibration set. All algorithms gave a very satisfactory result, with pricing differences with respect to their analytic calibration values less than 0.5 percent.

An important issue for the path-dependent lookback, barrier and digital barrier options above, is the frequency at which the stock price is observed for purposes of determining whether the barrier or its minimum level has been reached. In the numerical calculations below, we have assumed a discrete number of observations, namely at the close of each trading day. Moreover, we have assumed that a year consists of 250 trading days.

In Figure 3 we present simulation results with models for the digital barrier call option as a function of the barrier level (ranging from $1.05S_0$ to $1.5S_0$). As mentioned before, aside from the discounting factor e^{-rT} , the premiums can be interpreted as the chance of hitting the barrier during the option lifetime. In Figures 4-6, we show prices for all one-touch barrier options (as a percentage of the spot). The strike K was always taken equal to the spot S_0 . For reference we summarize in Table 9 all option prices for the above discussed exotics. One can check that the barrier results agree well with the identity $\text{DIB} + \text{DOB} = \text{vanilla call} = \text{UIB} + \text{UOB}$, suggesting that the simulation results are well converged. Lookback prices are presented in Table 3.

HEST	HESJ	BN-S	VG-CIR	VG-OUT	NIG-CIR	NIG-OUT
844.51	845.19	771.28	724.80	713.49	730.84	722.34

Table 3: Lookback Option prices

Consistently over all figures the Heston prices suggest that this model (for the current calibration) results in paths dynamics that are more *volatile*, breaching more frequently the imposed barriers. The results for the Lévy models with stochastic time change seem to move in pairs, with the choice of stochastic clock dominating over the details of the Lévy model upon which the stochastic time change is applied. The first couple, VG- Γ and NIG- Γ show very similar results, overall showing the least *volatile* path dynamics, whereas the VG-CIR and NIG-CIR prices consistently fall midway the pack. Finally the OU- Γ results without stochastic clock typically fall between the Heston and the VG-CIR and NIG-CIR prices.

Besides these qualitative observations it is important to note the magnitude of the observed differences. Lookback prices vary over about 15 percent, the one-touch barriers over 200 percent, whereas for the digital barriers we found price differences of over 10 percent.

For the cliquet options, the prices are shown in Figures 8-9 for two different combinations. The numerical values can be found in Tables 10 and 11. These results are in-line with the previous observations. Variations of over 40 percent are noted.

6 Pricing of Moment Derivatives

These derivatives depend on the realized higher moments of the underlying. More precisely, their payoff is a function of powers of the (daily) log-returns and allow to cover different kinds of market *shocks*. Variance swaps were already created to cover changes in the volatility regime. Besides the latter, skewness and kurtosis, also play an important role. To protect against a wrongly estimated skewness or kurtosis, moment derivatives of higher order can be useful. Recent studies by Corcuera, Nualart and Schoutens ([22], [23], [11] and [12]) suggest that functionals of powers of returns seem the natural choice to complete the market. It was shown that allowing trade in the power-assets of all orders in a incomplete Lévy market leads to a complete market. Power assets are strongly related to the realized higher moments and they mainly coincide in a discrete time framework [12].

6.1 Moment Swaps

Consider a finite set of discrete times $\{t_0 = 0, t_1, \dots, t_n = T\}$ at which the path of the underlying is monitored. We denote the price of the underlying at these points, i.e. S_{t_i} , by S_i for simplicity. Typically the t_i correspond to daily closing times and S_i is the closing price at day i . Note that then:

$$\log(S_i) - \log(S_{i-1}), \quad i = 1, \dots, n,$$

correspond to the daily log-returns. Next, we define the *moment swaps*. The k th-moment swap is a contract where the parties agree to exchange at maturity:

$$MOMS^{(k)} = N \times \left(\sum_{i=1}^n (\log(S_i) - \log(S_{i-1}))^k \right) = N \times \left(\sum_{i=1}^n \left(\log\left(\frac{S_i}{S_{i-1}}\right) \right)^k \right),$$

where N is the nominal amount.

A special case of these swaps is the second moment swap, better known as the Variance Swap. The non-centered payoff function in that case is given by:

$$VS = N \times \left(\sum_{i=1}^n (\log(S_i) - \log(S_{i-1}))^2 \right).$$

Basically this contract swaps fixed (annualized) variance by the realized variance (second moment) and as such provides protection against unexpected or unfavourable changes in volatility. Higher moment swaps provide the same kind of protection. The $MOMS^{(3)}$ is related to realized skewness and provides protection against changes in the symmetry of the underlying distribution. $MOMS^{(4)}$ derivatives are linked to realized kurtosis and provide protection against the unexpected occurrences of very large jumps, or in other words changes in the tail behaviour of the underlying distribution.

6.2 Moment Options

Related to the above discussed swaps, we define the associated options on the realized k th moment. More precisely, a *moment option* of order k , pays out at maturity T :

$$\left(\sum_{i=1}^n (\log(S_i/S_{i-1}))^k - K \right)^+.$$

The price of these options under risk-neutral valuation is given by:

$$MOMO^{(k)}(K, T) = \exp(-rT) E_Q \left[\left(\sum_{i=1}^n (\log(S_i/S_{i-1}))^k - K \right)^+ \right].$$

Note that since odd moments can be negative, the strike price for these options can range over the whole real line.

6.3 Hedging Moment Swaps

In line with the results obtained by Carr and Lewis [7], first consider the following (Taylor-like) expansion of the k th power of the logarithmic function:

$$(\log(x))^k = k! \left(x - 1 - \log(x) - \frac{(\log(x))^2}{2!} - \frac{(\log(x))^3}{3!} - \dots - \frac{(\log(x))^{k-1}}{(k-1)!} + \mathcal{O}((x-1)^{k+1}) \right).$$

Substituting x by S_i/S_{i-1} leads to:

$$(\log(S_i/S_{i-1}))^k = k! \left(\frac{\Delta S_i}{S_{i-1}} - \log(S_i/S_{i-1}) - \sum_{j=2}^{k-1} \frac{(\log(S_i/S_{i-1}))^j}{j!} + \mathcal{O}((\Delta S_i/S_{i-1})^{k+1}) \right),$$

where $\Delta S_i = S_i - S_{i-1}$.

Summing over i gives a decomposition of the $MOMS^{(k)}$ payoff:

$$\begin{aligned} MOMS^{(k)} &= N \sum_{i=1}^n (\log(S_i/S_{i-1}))^k \\ &= Nk! \sum_{i=1}^n \left(\frac{\Delta S_i}{S_{i-1}} - \log(S_i/S_{i-1}) - \sum_{j=2}^{k-1} \frac{(\log(S_i/S_{i-1}))^j}{j!} + \mathcal{O}((\Delta S_i/S_{i-1})^{k+1}) \right) \\ &= -Nk! (\log(S_T) - \log(S_0)) \\ &\quad + Nk! \sum_{i=1}^n \frac{\Delta S_i}{S_{i-1}} - N \sum_{j=2}^{k-1} \frac{k!}{j!} MOMS^{(j)} + \mathcal{O}\left(\sum_{i=1}^n (\Delta S_i/S_{i-1})^{k+1}\right) \end{aligned} \quad (11)$$

Thus up to $(k+1)$ th-order terms the sum of the k th powered log-returns decomposes into the payouts from:

- a log-contract $(-k! (\log(S_T) - \log(S_0)))$;

- a dynamic strategy ($k! \sum_{i=1}^n \frac{\Delta S_i}{S_{i-1}}$);
- a series of moment contracts of order strictly smaller than k .

The log-contract itself can be hedged by a static position in the underlying, in a bond and in a (discrete approximation of a continuous) set of European vanilla call and put options maturing at time T . More precisely, first note that for any $L > 0$:

$$\log(S_T) - \log(S_0) = \frac{1}{L}(S_T - S_0) - u(S_T) + u(S_0), \quad (12)$$

for:

$$u(S) = \left(\frac{S - L}{L} - \log(S) + \log(L) \right).$$

Moreover Carr and Lewis [7] show that:

$$u(S_T) = \int_0^L \frac{1}{K^2} (K - S_T)^+ dK + \int_L^{+\infty} \frac{1}{K^2} (S_T - K)^+ dK. \quad (13)$$

Since $S_T - S_0 = \sum_{i=1}^n \Delta S_i$, substituting (13) in (12) and (11) implies:

$$\begin{aligned} MOMS^{(k)} \approx & Nk! \left(\int_0^L \frac{1}{K^2} (K - S_T)^+ dK + \int_L^{+\infty} \frac{1}{K^2} (S_T - K)^+ dK \right) \\ & + N \left(k! \sum_{i=1}^n \left(\frac{1}{S_{i-1}} - \frac{1}{L} \right) \Delta S_i - k! u(S_0) - \sum_{j=2}^{k-1} \frac{k!}{j!} MOMS^{(j)} \right) \end{aligned}$$

6.4 Pricing of Moments Swaps

We calculate under the different models, the risk-neutral expectation:

$$E_Q \left[MOMS^{(k)} \right],$$

We consistently average over 1.000.000 simulated paths. All options have a lifetime of 1 year. In Table 4, we clearly see how the price differences are even more pronounced as compared to the exotic option pricings discussed in section 5.2.

	order	HEST	BN-S	VG-CIR	VG-OUF	NIG-CIR	NIG-OUF
$e^{-rT} E_Q$	$MOMS^{(2)}$	623.89	804.60	557.55	628.85	557.75	641.71
$e^{-rT} E_Q$	$MOMS^{(3)}$	-0.0807	-312.58	-21.03	-74.91	-21.69	-88.82
$e^{-rT} E_Q$	$MOMS^{(4)}$	0.6366	322.40	7.8698	33.89	8.554	47.99

Table 4: Moment swaps ($N = 10000$)

6.5 Pricing of Moments Options

Next, we calculate the prices of moment call option, $MOMO^{(k)}$, paying out at maturity T :

$$\left(\sum_{i=1}^n (\log(S_i/S_{i-1}))^k - K \right)^+,$$

the price of these call moment options is by the risk-neutral valuation:

$$MOMO^{(k)}(K, T) = \exp(-rT) E_Q \left[\sum_{i=1}^n (\log(S_i/S_{i-1}))^k - K \right]^+.$$

We plot in Figures 10-12 the prices over a whole range of strikes and the corresponding values can be found in Tables 5-7.

K (in bp)	HEST	BN-S	VG-CIR	VG-OUT	NIG-CIR	NIG-OUT
100	302.3301	491.4817	212.0101	183.3647	249.068	161.5099
200	219.1410	436.4667	152.6484	121.4477	186.381	100.5233
300	156.7058	394.0581	110.6050	83.4256	140.753	67.6916
400	109.5242	357.8177	80.4430	58.7503	106.257	47.7753
500	75.9747	326.6175	58.2142	42.1646	80.235	35.2828
600	52.4440	300.0791	42.2200	31.0541	60.917	26.9061
700	37.0312	277.1135	30.0486	23.5572	46.407	20.2450
800	25.9978	256.4670	21.2445	17.9608	36.175	15.0211
900	17.4472	238.1357	14.8481	14.1807	28.402	11.2782
1000	11.2276	221.1757	10.4386	11.1815	24.19	8.4718

Table 5: Moment option of order 2 (N=10000)

The disparity between the models is amplified. The Lévy models with stochastic time change seem again to move in the same pairs as in agreement with results in section 5.2, but now only up to the third order moment option. The BNS model has very pronounced second and fourth order moment option prices, while HEST drops (in absolute value) to very low values for the fourth order moment option compared to the other models.

7 Conclusion

We have looked at different models, all reflecting non-normal returns and stochastic volatility. Empirical work has generally supported the need for both ingredients.

We have demonstrated the clear ability of all proposed processes to produce a very convincing fit to a market-conform volatility surface. At the same time we have shown that this calibration could be achieved in a timely manner using a very fast computational procedure based on FFT.

K	HEST	BN-S	VG-CIR	VG-OUT	NIG-CIR	NIG-OUT
-0.010	98.0459	79.9869	89.5862	84.6786	87.4962	82.2679
-0.009	88.2341	71.3740	79.9497	75.1442	78.1320	72.8796
-0.008	78.4223	62.8212	70.3448	65.6663	68.8121	63.5948
-0.007	68.6105	54.3490	60.8159	56.2683	59.5498	54.3998
-0.006	58.7987	46.0100	51.3447	46.9840	50.3831	45.3475
-0.005	48.9869	37.7781	41.9813	37.8554	41.3352	36.4821
-0.004	39.1751	29.6576	32.7639	28.9710	32.4824	27.8108
-0.003	29.3686	21.7306	23.7993	20.3739	23.8966	19.4166
-0.002	19.5673	14.0430	15.3273	12.3057	15.6840	11.4694
-0.001	9.8393	6.6657	7.5947	5.3112	8.1994	4.4442
0.000	0.7274	0.0997	1.9022	0.8162	2.4520	0.1462
0.001	0.0008	0	0.8012	0.2915	1.1520	0.0173
0.002	0	0	0.4866	0.1559	0.6438	0.0074
0.003	0	0	0.3267	0.0938	0.4213	0
0.004	0	0	0.2293	0.0486	0.2819	0
0.005	0	0	0.1614	0.0322	0.1998	0
0.006	0	0	0.1052	0.0224	0.1325	0
0.007	0	0	0.0648	0.0126	0.0873	0
0.008	0	0	0.0416	0.0028	0.0578	0
0.009	0	0	0.0268	0	0.0287	0
0.010	0	0	0.0170	0	0.0091	0

Table 6: Moment option of order 3 (N=10000)

Note, that an almost identical calibration means that at the time-points of the maturities of the calibration data set the marginal distribution is fitted accurately to the risk-neutral distribution implied by the market. If we have different models leading all to such almost perfect calibrations, all models have almost the same marginal distributions. It should however be clear that even if at all time-points $0 \leq t \leq T$ marginal distributions among different models coincide, this does not imply that exotic prices should also be the same. This can be seen from the following discrete-time example. Let $n \geq 2$ and $X = \{X_i, i = 1, \dots, n\}$ be an iid sequence and let $\{u_i, i = 1, \dots, n\}$ be an independent sequence which randomly varies between $u_i = 0$ and 1. We propose two discrete (be it unrealistic) stock price models, $S^{(1)}$ and $S^{(2)}$, with the same marginal distributions:

$$S_i^{(1)} = u_i X_1 + (1 - u_i) X_2 \text{ and } S_i^{(2)} = X_i$$

The first process flips randomly between two states X_1 and X_2 , both of which follow the distribution of the iid sequence, and so do all the marginals at the time points $i = 1, \dots, n$. The second process changes value in all time points. The values are independent of each other and all follow again the same distribution of the iid sequence. In both cases all the marginal distributions (at every $i = 1, \dots, n$) are the same (as the distribution underlying the sequence X). It is clear however that the maximum and minimum of both processes behave completely

K	HEST	BN-S	VG-CIR	VG-OUT	NIG-CIR	NIG-OUT
0.0001	0.0781	35.7465	1.9322	2.3416	5.2360	3.6095
0.0002	0.0259	35.4823	1.5977	2.0015	4.8754	3.3309
0.0003	0.0120	35.2471	1.3603	1.7655	4.6077	3.1274
0.0004	0.0065	35.0274	1.1821	1.5879	4.3995	2.9601
0.0005	0.0033	34.8220	1.0428	1.4542	4.2249	2.8158
0.0006	0.0011	34.6307	0.9281	1.3386	4.0755	2.6878
0.0007	0.0001	34.4525	0.8328	1.2403	3.9403	2.5750
0.0008	0	34.2810	0.7506	1.1552	3.8221	2.4746
0.0009	0	34.1127	0.6790	1.0805	3.7211	2.3819
0.0010	0	33.9479	0.6202	1.0160	3.6303	2.2979

Table 7: Moment option of order 4 (N=10000)

different. For the first process, the maximal $\max_{j \leq i} S_i^{(1)} = \max(X_1, X_2)$ and minimal process $\min_{j \leq i} S_i^{(1)} = \min(X_1, X_2)$ for i large enough, whereas for the second process there is much more variation possible and it clearly leads to other distributions. In summary, it should be clear that equal marginal distributions of a process do not at all imply equal marginal distributions of the associated minimal or maximal process. This explains why matching European call prices do not lead necessarily to matching exotic prices. It is the underlying fine-grain structure of the process that will have an important impact on the path-dependent option prices.

We have illustrated this by pricing exotics by Monte-Carlo simulation, showing that price differences for one-touch barriers of over 200 percent are no exception. For lookback call options a price range of more than 15 percent amongst the models was observed. A similar conclusion was valid for the digital barrier premiums. Even for cliquet options, which only depend on the stock realisations over a limited amount of time-points, prices vary substantially among the models. Moment derivatives amplify pricing disparity. At the same time the presented details of the Monte-Carlo implementation should allow the reader to embark on his/her own pricing experiments.

The conclusion is that great care should be taken when employing attractive fancy-dancy models to price (or even more important, to evaluate hedge parameters for) exotics. As far as we know no detailed study about the underlying path structure of assets has been done yet. Our study motivates such a deeper investigation.

Acknowledgments

The first author is a Postdoctoral Fellow of the Fund for Scientific Research - Flanders (Belgium) (F.W.O. - Vlaanderen). We thank Marc Jeannin for his devoted programming work.

References

- [1] Bakshi, G., Cao, C. and Chen, Z. (1997): *Empirical Performance of Alternative Option Pricing Models*, The Journal of Finance, Vol. LII, No. 5, 2003-2049.
- [2] Barndorff-Nielsen, O.E. and Shephard, N. (2001): *Non-Gaussian Ornstein–Uhlenbeck-based Models and Some of Their Uses in Financial Economics*, Journal of the Royal Statistical Society, Series B **63**, 167–241.
- [3] Barndorff-Nielsen, O.E., Nicolata, E. and Shephard, N. (2002): *Some Recent Developments in Stochastic Volatility Modelling*, Quantitative Finance **2**, 11–23.
- [4] Beine, M., Laurent, S. and Palm, F.C. (2004): *Central Bank Forex Interventions Assessed Using Realized Moments*, CORE Discussion paper 2004/1.
- [5] Bertoin, J. (1996): *Lévy Processes*, Cambridge Tracts in Mathematics **121**, Cambridge University Press, Cambridge.
- [6] Black, F. and Scholes, M. (1973): *The Pricing of Options and Corporate Liabilities*, Journal of Political Economy, **81**, 637–654.
- [7] Carr, P. and Lewis, K. (2004): *Corridor Variance Swaps*, Risk Magazine, **17-2**, February 2004, 67–72.
- [8] Carr, P. and Madan, D. (1998): *Option Valuation Using the Fast Fourier Transform*, Journal of Computational Finance **2**, 61–73.
- [9] Carr, P., Geman, H., Madan, D.H. and Yor, M. (2001): *Stochastic Volatility for Lévy Processes*, Prépublications du Laboratoire de Probabilités et Modèles Aléatoires **645**, Universités de Paris 6 & Paris 7, Paris.
- [10] Clark, P. (1973): *A Subordinated Stochastic Process Model with Finite Variance for Speculative Prices*, Econometrica **41**, 135–156.
- [11] Corcuera, J.M., Nualart, D. and Schoutens, W. (2004): *Completion of a Lévy Market by Power- Jump Assets*, Finance and Stochastics, to appear.
- [12] Corcuera, J.M., Nualart, D. and Schoutens, W. (2004): *Moment Derivatives and Lévy-type Market Completion*, this volume.
- [13] Cox, J., Ingersoll, J. and Ross, S. (1985): *A Theory of the Term Structure of Interest Rates*, Econometrica **53**, 385–408.
- [14] Dacorogna, M.M., Gençay, R., Müller, U., Olsen, R.B. and Pictet, O.V. (2001): *An Introduction to High Frequency Finance*, Academic Press, San Diego.

- [15] Devroye, L. (1986): *Non-Uniform Random Variate Generation*, Springer-Verlag, New York.
- [16] Heston, S. (1993): *A closed-form solution for options with stochastic volatility with applications to bond and currency options*, Review of Financial Studies **6**, 327-343.
- [17] Hirsa, A., Courtadon, G. and Madan, B.D. (2003): *The Effect of Model Risk on the Valuation of Barrier Options*, The Journal of Risk Finance, Winter 2003, 1–8.
- [18] Hull, J. and Suo, W. (2001): *A Methodology for Assessing Model Risk and its Application to the Implied Volatility Function Model*, Working Paper University of Toronto, Canada, July 2001.
- [19] Jäckel, P. (2002): *Monte Carlo Methods in Finance*, Wiley.
- [20] Knudsen, Th. and Nguyen-Ngoc, L. (2003): *Pricing European Options in a Stochastic Volatility-Jump-Diffusion Model*, working paper.
- [21] Madan, D.B., Carr, P. and Chang, E.C. (1998): *The Variance Gamma Process and Option Pricing*, European Finance Review **2**, 79–105.
- [22] Nualart, D. and Schoutens W. (2000): *Chaotic and Predictable Representations for Lévy Processes*, Stochastic Processes and their Application, **90**(1), 109–122.
- [23] Nualart, D. and Schoutens W. (2001): *Backwards Stochastic Differential Equations and Feynman-Kac Formula for Lévy Processes with Applications in Finance*, Bernoulli, **7**(5), 761–776.
- [24] Schoutens, W. (2003): *Lévy Processes in Finance: Pricing Financial Derivatives*, Wiley.
- [25] Schoutens, W., Simons E. and Tistaert, J. (2004), *A Perfect Calibration ! Now What ?*, Wilmott Magazine, March 2004.
- [26] Wilmott, P. (2002): *Cliquet Options and Volatility Models*, Wilmott Magazine, December 2002.

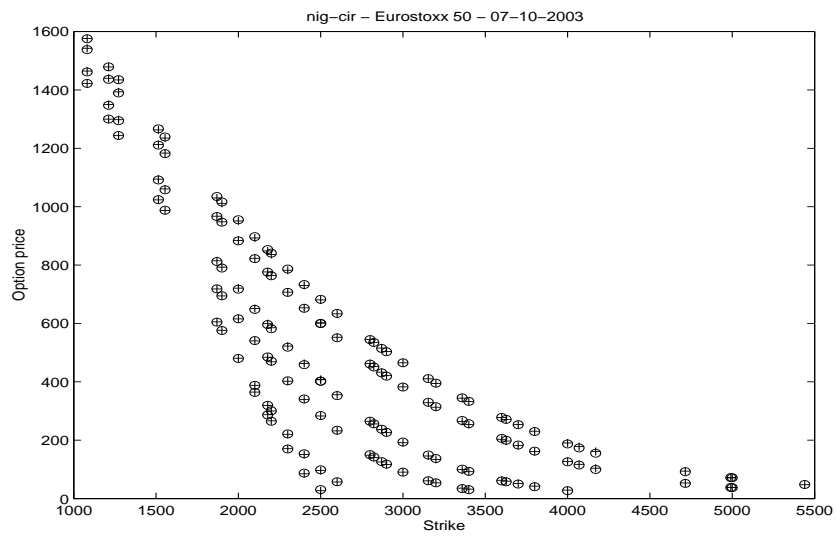


Figure 1: Calibration of NIG-CIR Model

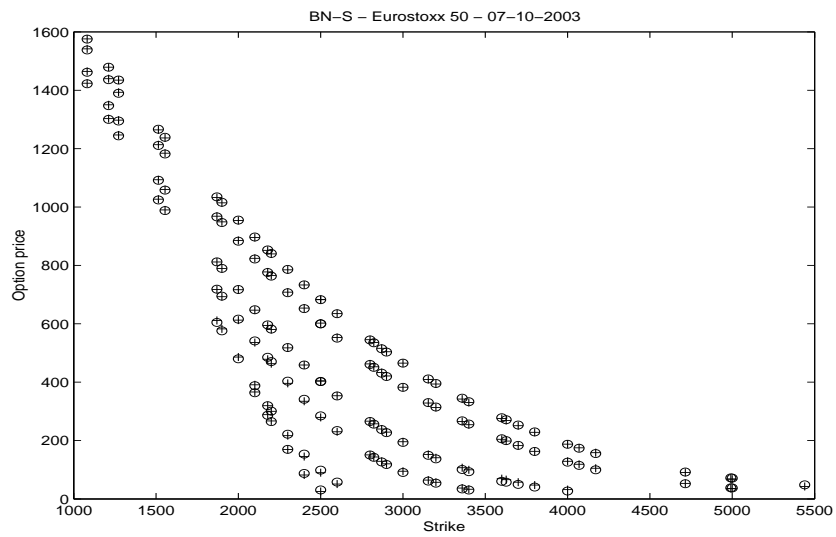


Figure 2: Calibration of Barndorff-Nielsen-Shephard Model

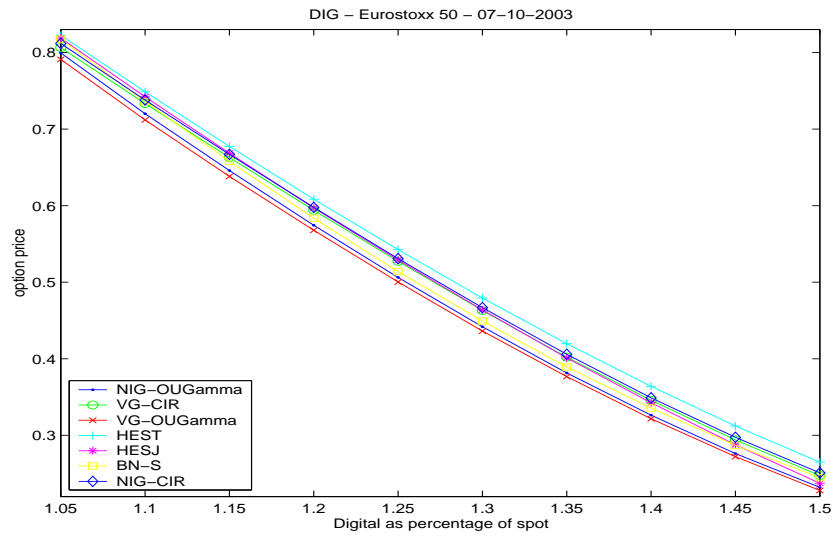


Figure 3: Digital Barrier prices

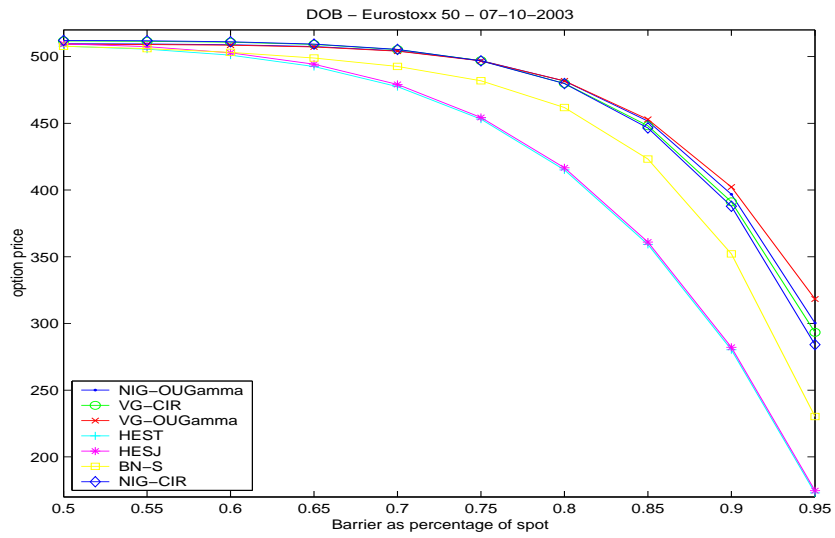


Figure 4: DOB prices

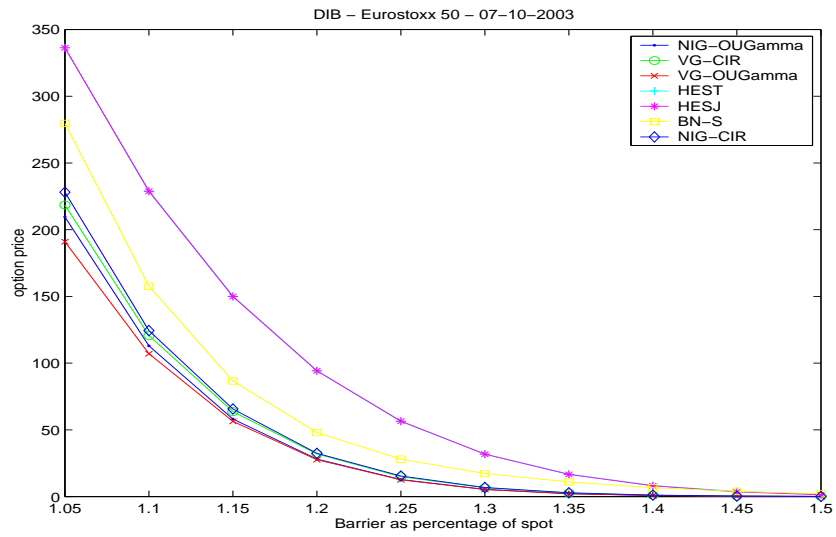


Figure 5: DIB prices

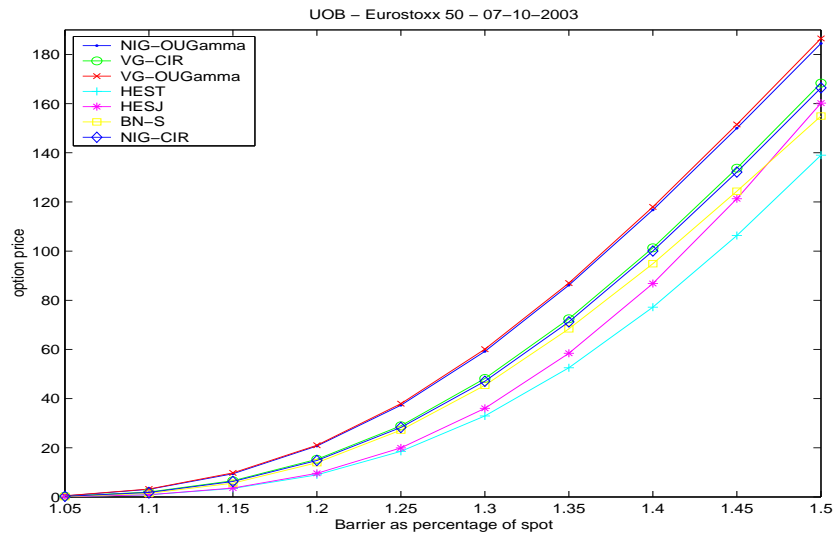


Figure 6: UOB prices

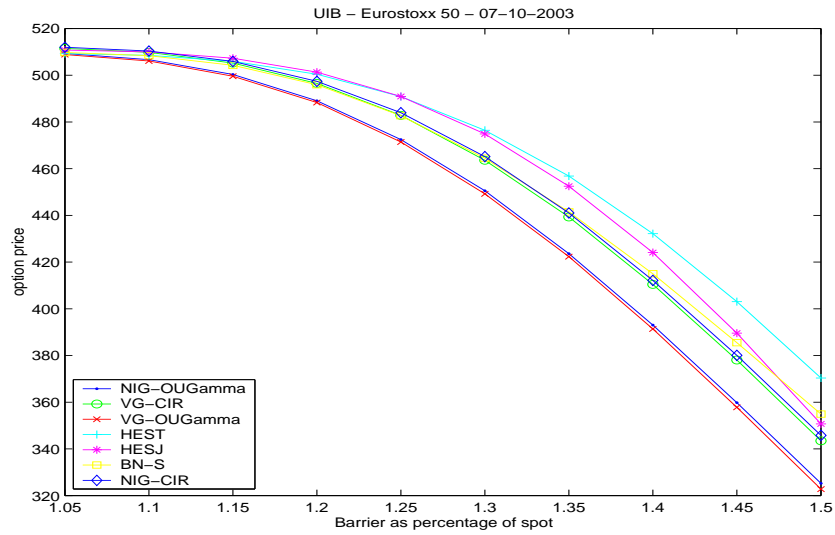


Figure 7: UIB prices

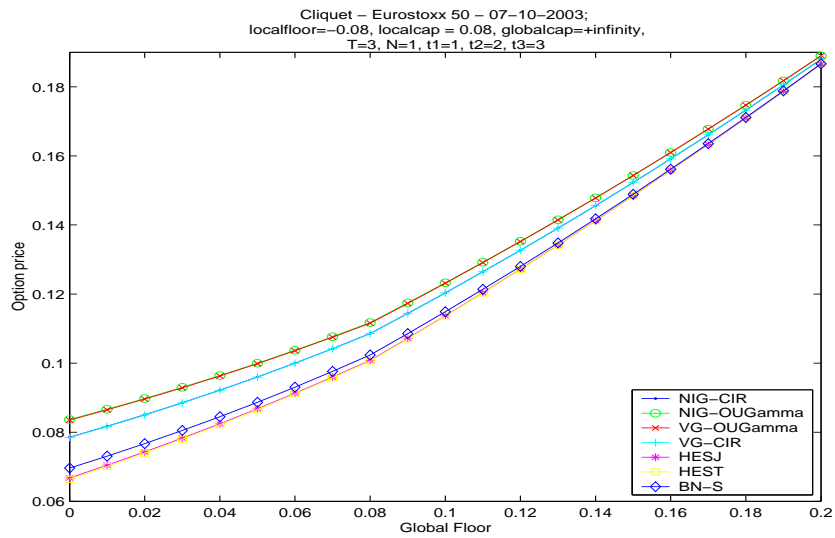


Figure 8: Cliquet prices: $cap_{loc} = 0.08$, $flo_{loc} = -0.08$, $cap_{glo} = +\infty$, $N = 3$, $t_1 = 1, t_2 = 2, t_3 = 3$

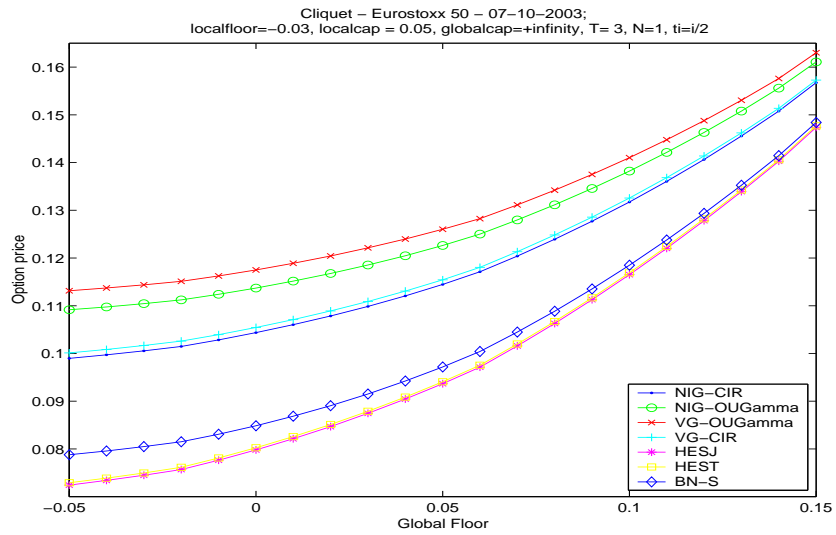


Figure 9: Cliquet Prices: $fl_{loc} = -0.03$, $cap_{loc} = 0.05$, $cap_{glo} = +\infty$, $T = 3$, $N = 6$, $t_i = i/2$

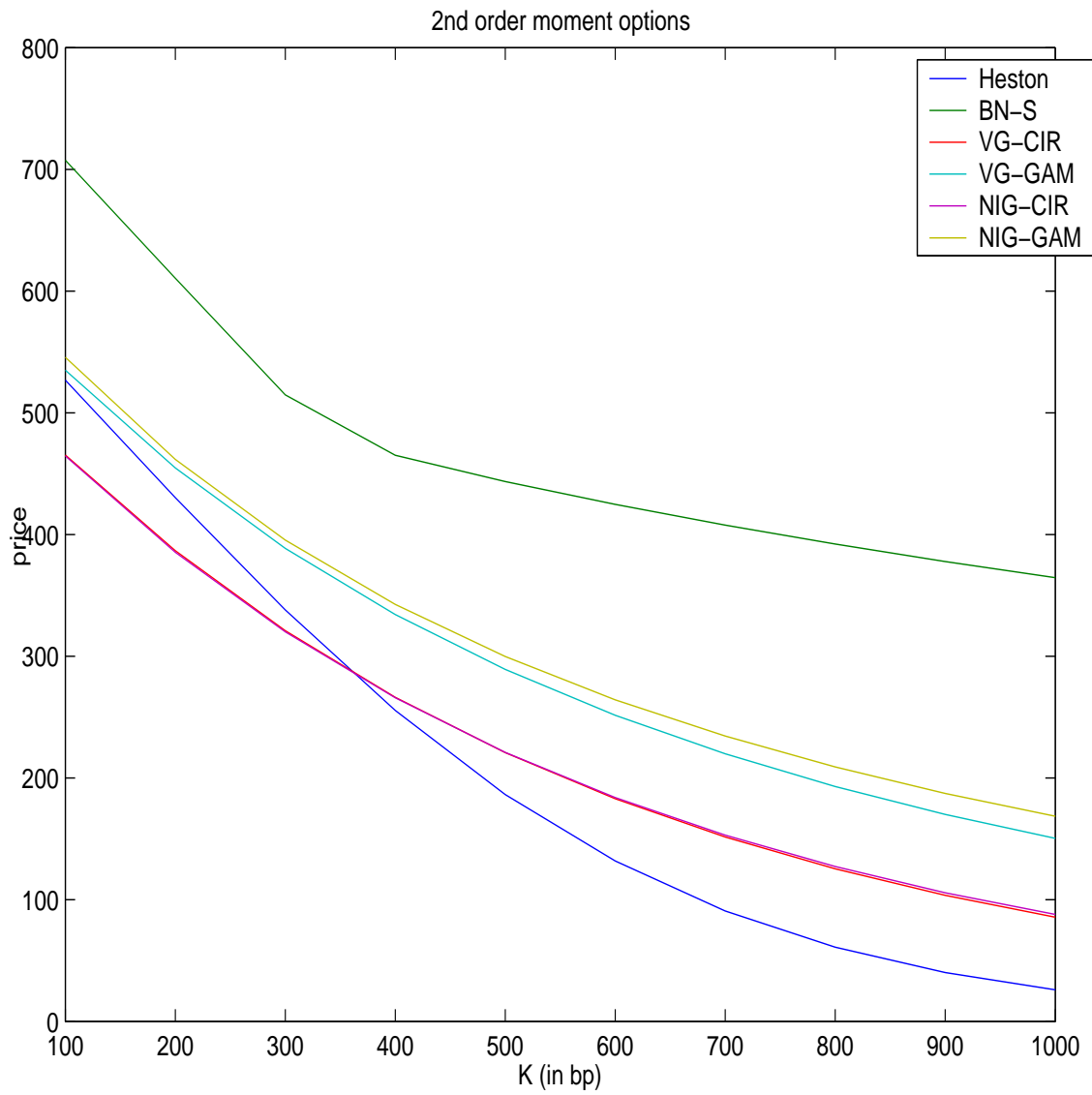


Figure 10: Moment option of 2nd order

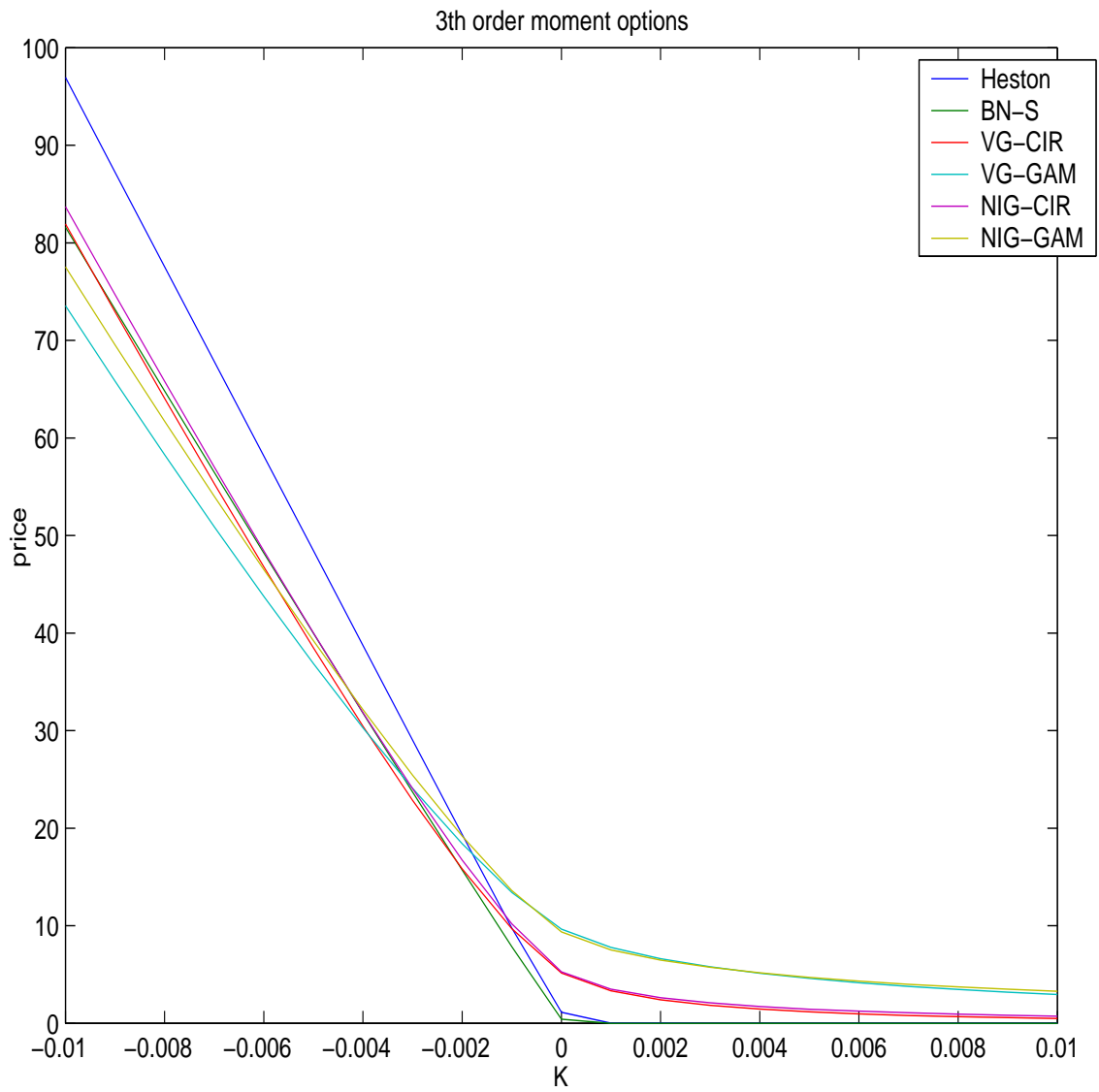


Figure 11: Moment option of 3th order

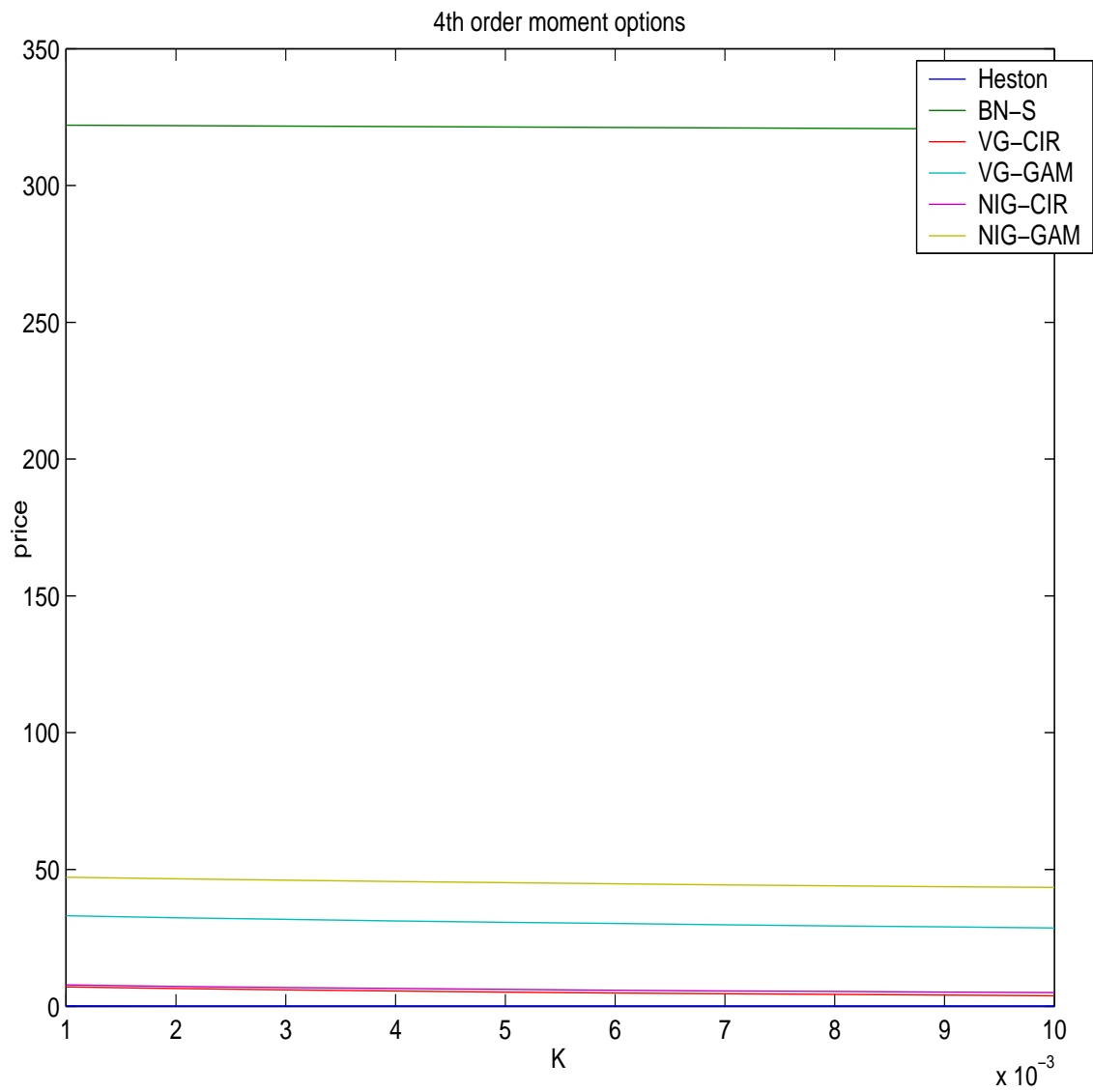


Figure 12: Moment option of 4th order

Maturity (yearfraction)	0.0361	0.2000	1.1944	2.1916	4.2056	5.1639
Strike						
1081.82			0.3804	0.3451	0.3150	0.3137
1212.12			0.3667	0.3350	0.3082	0.3073
1272.73			0.3603	0.3303	0.3050	0.3043
1514.24			0.3348	0.3116	0.2920	0.2921
1555.15			0.3305	0.3084	0.2899	0.2901
1870.30		0.3105	0.2973	0.2840	0.2730	0.2742
1900.00		0.3076	0.2946	0.2817	0.2714	0.2727
2000.00		0.2976	0.2858	0.2739	0.2660	0.2676
2100.00	0.3175	0.2877	0.2775	0.2672	0.2615	0.2634
2178.18	0.3030	0.2800	0.2709	0.2619	0.2580	0.2600
2200.00	0.2990	0.2778	0.2691	0.2604	0.2570	0.2591
2300.00	0.2800	0.2678	0.2608	0.2536	0.2525	0.2548
2400.00	0.2650	0.2580	0.2524	0.2468	0.2480	0.2505
2499.76	0.2472	0.2493	0.2446	0.2400	0.2435	0.2463
2500.00	0.2471	0.2493	0.2446	0.2400	0.2435	0.2463
2600.00		0.2405	0.2381	0.2358	0.2397	0.2426
2800.00			0.2251	0.2273	0.2322	0.2354
2822.73			0.2240	0.2263	0.2313	0.2346
2870.83			0.2213	0.2242	0.2295	0.2328
2900.00			0.2198	0.2230	0.2288	0.2321
3000.00			0.2148	0.2195	0.2263	0.2296
3153.64			0.2113	0.2141	0.2224	0.2258
3200.00			0.2103	0.2125	0.2212	0.2246
3360.00			0.2069	0.2065	0.2172	0.2206
3400.00			0.2060	0.2050	0.2162	0.2196
3600.00				0.1975	0.2112	0.2148
3626.79				0.1972	0.2105	0.2142
3700.00				0.1964	0.2086	0.2124
3800.00				0.1953	0.2059	0.2099
4000.00				0.1931	0.2006	0.2050
4070.00					0.1988	0.2032
4170.81					0.1961	0.2008
4714.83					0.1910	0.1957
4990.91					0.1904	0.1949
5000.00					0.1903	0.1949
5440.18						0.1938

Table 8: Implied Volatility Surface EUROSTOXX 50, Oct 7th 2003

	H/S_0	NIG- OUT	VG- CIR	VG- -OUT	HEST	HESJ	BN-S	NIG- CIR
LC		722.34	724.80	713.49	844.51	845.18	771.28	730.84
Call		509.76	511.80	509.33	510.88	510.89	509.89	512.21
DOB	0.95	300.25	293.28	318.35	173.85	174.64	230.25	284.10
DOB	0.9	396.80	391.17	402.24	280.79	282.09	352.14	387.83
DOB	0.85	451.61	448.10	452.97	359.05	360.99	423.21	446.52
DOB	0.8	481.65	479.83	481.74	414.65	416.63	461.82	479.77
DOB	0.75	497.00	496.95	496.80	452.76	454.33	481.85	496.78
DOB	0.7	504.31	505.24	504.05	477.37	479.12	492.62	505.38
DOB	0.65	507.53	509.10	507.21	492.76	494.25	498.93	509.34
DOB	0.6	508.88	510.75	508.53	501.74	502.84	503.17	511.09
DOB	0.55	509.43	511.40	509.06	506.46	507.41	505.93	511.80
DOB	0.5	509.64	511.67	509.24	508.91	509.51	507.68	512.08
DIB	0.95	209.51	218.51	190.98	337.03	336.25	279.61	228.10
DIB	0.9	112.95	120.62	107.08	230.09	228.80	157.72	124.37
DIB	0.85	58.14	63.69	56.35	151.83	149.90	86.65	65.68
DIB	0.8	28.11	31.96	27.59	96.24	94.26	48.04	32.43
DIB	0.75	12.76	14.84	12.53	58.13	56.56	28.01	15.42
DIB	0.7	5.45	6.55	5.28	33.51	31.77	17.24	6.83
DIB	0.65	2.23	2.70	2.11	18.12	16.64	10.94	2.87
DIB	0.6	0.88	1.04	0.79	9.14	8.05	6.69	1.11
DIB	0.55	0.33	0.39	0.26	4.42	3.48	3.94	0.40
DIB	0.5	0.12	0.13	0.09	1.98	1.38	2.19	0.13
UIB	1.05	509.32	511.52	508.84	510.78	510.81	509.73	511.98
UIB	1.1	506.68	509.80	506.11	500.90	510.00	508.38	510.37
UIB	1.15	500.33	505.21	499.56	507.08	507.28	504.28	505.93
UIB	1.2	489.05	496.50	488.30	501.04	501.31	495.95	497.41
UIB	1.25	472.47	482.84	471.39	490.73	490.93	482.66	483.94
UIB	1.3	450.54	463.62	449.23	475.30	474.86	464.48	465.16
UIB	1.35	423.62	439.32	422.32	454.77	452.47	441.48	441.00
UIB	1.4	393.01	410.46	391.36	428.96	424.09	414.98	412.16
UIB	1.45	359.77	378.05	357.80	399.24	389.56	385.50	380.04
UIB	1.5	325.25	343.46	322.79	365.57	350.68	354.90	345.79
UOB	1.05	0.44	0.27	0.49	0.103	0.08	0.13	0.23
UOB	1.1	3.08	2.00	3.22	0.979	0.89	1.48	1.84
UOB	1.15	9.43	6.59	9.77	3.80	3.61	5.58	6.27
UOB	1.2	20.71	15.29	21.03	8.96	9.85	13.91	14.80
UOB	1.25	37.29	28.95	37.94	20.15	19.96	27.20	28.26
UOB	1.3	59.22	48.17	60.10	35.58	36.03	45.38	47.04
UOB	1.35	86.14	72.47	87.00	56.10	58.42	68.39	71.21
UOB	1.4	116.75	101.33	117.96	81.93	86.80	94.88	100.04
UOB	1.45	149.98	133.74	151.52	111.65	121.33	124.36	132.16
UOB	1.5	184.50	168.33	186.53	145.31	160.21	154.96	166.41
DIG	1.05	0.7995	0.8064	0.7909	0.8218	0.8189	0.8173	0.8118
DIG	1.1	0.7201	0.7334	0.7120	0.7478	0.7421	0.7360	0.7380
DIG	1.15	0.6458	0.6628	0.6382	0.6762	0.6685	0.6580	0.6670
DIG	1.2	0.5744	0.5940	0.5678	0.6069	0.5971	0.5836	0.5977
DIG	1.25	0.5062	0.5273	0.5003	0.5408	0.5290	0.5138	0.5308
DIG	1.3	0.4418	0.4630	0.4363	0.4769	0.4637	0.4493	0.4668
DIG	1.35	0.3816	0.4021	0.3767	0.4169	0.4012	0.3893	0.4059
DIG	1.4	0.3264	0.3456	0.3217	0.3603	0.3426	0.3355	0.3490
DIG	1.45	0.2763	0.2940	0.2722	0.3087	0.2877	0.2870	0.2975
DIG	1.5	0.2321	0.2474	0.2280	0.2610	0.2374	0.2446	0.2510

Table 9: Exotic Option prices

flo_{glo}	NIG- CIR	NIG- OUT	VG- -OUT	VG- CIR	HESJ	HEST	BN-S
0.00	0.0785	0.0837	0.0835	0.0785	0.0667	0.0683	0.0696
0.01	0.0817	0.0866	0.0865	0.0817	0.0704	0.0719	0.0731
0.02	0.0850	0.0897	0.0896	0.0850	0.0743	0.0757	0.0767
0.03	0.0885	0.0930	0.0928	0.0885	0.0783	0.0796	0.0805
0.04	0.0922	0.0964	0.0963	0.0921	0.0825	0.0837	0.0845
0.05	0.0960	0.1000	0.0998	0.0960	0.0868	0.0879	0.0887
0.06	0.1000	0.1037	0.1036	0.1000	0.0913	0.0923	0.0930
0.07	0.1042	0.1076	0.1075	0.1042	0.0959	0.0969	0.0976
0.08	0.1086	0.1117	0.1116	0.1085	0.1008	0.1017	0.1024
0.09	0.1144	0.1174	0.1173	0.1144	0.1072	0.1080	0.1085
0.10	0.1203	0.1232	0.1231	0.1203	0.1137	0.1145	0.1149
0.11	0.1264	0.1292	0.1291	0.1264	0.1204	0.1211	0.1214
0.12	0.1327	0.1353	0.1352	0.1327	0.1272	0.1279	0.1280
0.13	0.1391	0.1415	0.1414	0.1391	0.1342	0.1348	0.1348
0.14	0.1456	0.1478	0.1478	0.1456	0.1412	0.1418	0.1418
0.15	0.1523	0.1543	0.1543	0.1523	0.1485	0.1489	0.1489
0.16	0.1591	0.1610	0.1610	0.1591	0.1558	0.1562	0.1561
0.17	0.1661	0.1677	0.1678	0.1661	0.1633	0.1637	0.1635
0.18	0.1732	0.1747	0.1747	0.1733	0.1709	0.1712	0.1711
0.19	0.1805	0.1817	0.1818	0.1806	0.1787	0.1789	0.1788
0.20	0.1880	0.1889	0.1890	0.1880	0.1866	0.1868	0.1867

Table 10: Cliquet prices: $cap_{loc} = 0.08$, $flo_{-loc} = 0.08$, $cap_{glo} = +\infty$, $flo_{glo} \in [0, 0.20]$, $N = 3$, $t_1 = 1$, $t_2 = 2$, $t_3 = 3$

flo_{glo}	NIG- CIR	NIG- OUT	VG- -OUT	VG- CIR	HESJ	HEST	BN-S
-0.05	0.0990	0.1092	0.1131	0.1001	0.0724	0.0762	0.0788
-0.04	0.0997	0.1098	0.1137	0.1008	0.0734	0.0771	0.0796
-0.03	0.1005	0.1104	0.1144	0.1017	0.0745	0.0781	0.0805
-0.02	0.1015	0.1112	0.1151	0.1026	0.0757	0.0762	0.0815
-0.01	0.1028	0.1124	0.1162	0.1039	0.0776	0.0811	0.0831
0.00	0.1044	0.1137	0.1175	0.1054	0.0798	0.0831	0.0849
0.01	0.1060	0.1152	0.1189	0.1071	0.0821	0.0853	0.0869
0.02	0.1079	0.1168	0.1204	0.1089	0.0847	0.0877	0.0891
0.03	0.1099	0.1185	0.1221	0.1109	0.0874	0.0904	0.0915
0.04	0.1121	0.1205	0.1240	0.1131	0.0904	0.0932	0.0942
0.05	0.1145	0.1226	0.1260	0.1154	0.0937	0.0963	0.0972
0.06	0.1171	0.1250	0.1283	0.1180	0.0971	0.0996	0.1004
0.07	0.1204	0.1280	0.1311	0.1213	0.1016	0.1039	0.1045
0.08	0.1239	0.1312	0.1342	0.1248	0.1063	0.1084	0.1088
0.09	0.1277	0.1346	0.1375	0.1286	0.1113	0.1132	0.1135
0.10	0.1317	0.1382	0.1410	0.1326	0.1165	0.1183	0.1185
0.11	0.1361	0.1421	0.1448	0.1368	0.1220	0.1237	0.1238
0.12	0.1406	0.1463	0.1488	0.1414	0.1278	0.1293	0.1294
0.13	0.1456	0.1508	0.1531	0.1462	0.1339	0.1352	0.1353
0.14	0.1508	0.1556	0.1576	0.1514	0.1403	0.1415	0.1415
0.15	0.1567	0.1611	0.1630	0.1573	0.1474	0.1484	0.1484

Table 11: Cliquet Prices: $flo_{loc} = -0.03$, $cap_{loc} = 0.05$, $cap_{glo} = +\infty$, $T = 3$, $N = 6$, $t_i = i/2$